

Accepted Manuscript

Increased production of 27-hydroxycholesterol in human colorectal cancer advanced stage: Possible contribution to cancer cell survival and infiltration

D. Rossin, I.H.K. Dias, M. Solej, I. Milic, A.R. Pitt, N. Iaia, L. Scoppapietra, A. Devitt, M. Nano, M. Degiuli, M. Volante, C. Caccia, V. Leoni, H.R. Griffiths, C.M. Spickett, G. Poli, F. Biasi

PII: S0891-5849(19)30266-7

DOI: <https://doi.org/10.1016/j.freeradbiomed.2019.03.020>

Reference: FRB 14205

To appear in: *Free Radical Biology and Medicine*

Received Date: 20 February 2019

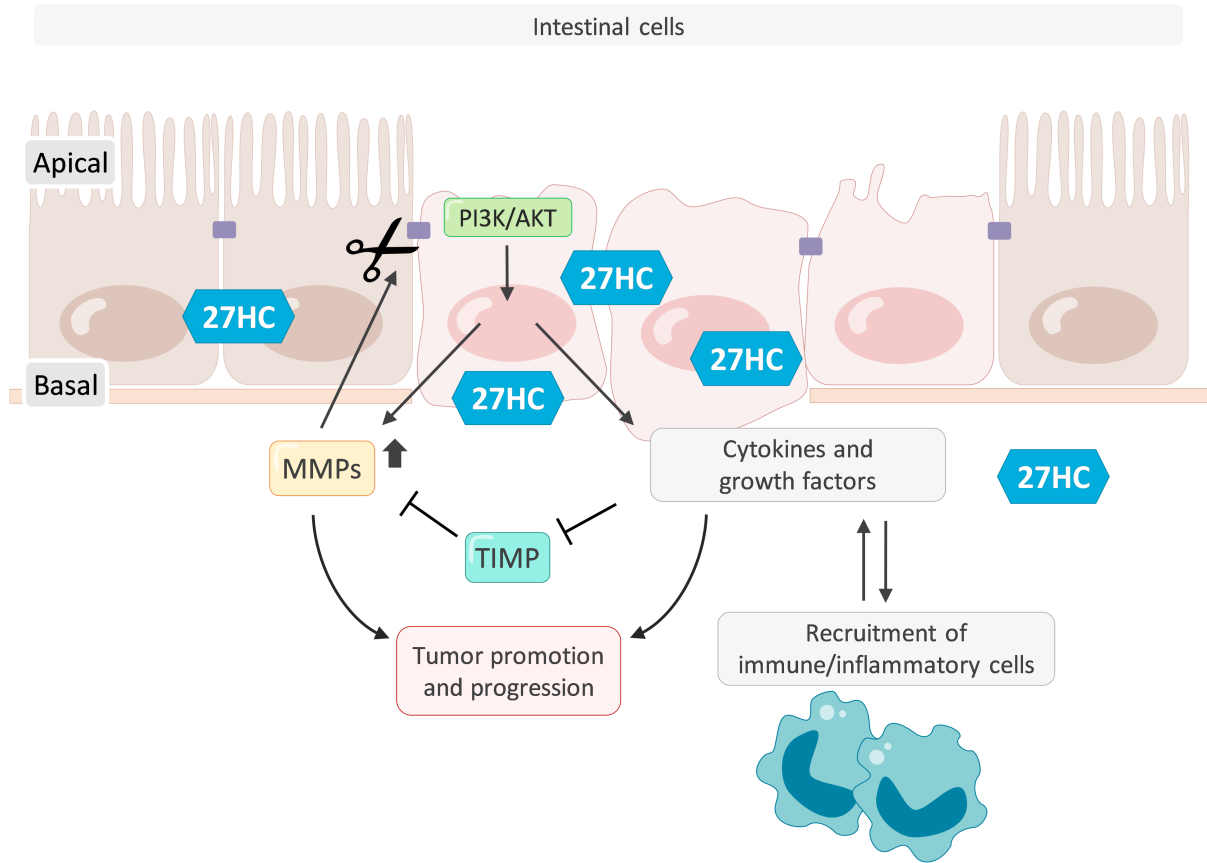
Revised Date: 15 March 2019

Accepted Date: 18 March 2019

Please cite this article as: D. Rossin, I.H.K. Dias, M. Solej, I. Milic, A.R. Pitt, N. Iaia, L. Scoppapietra, A. Devitt, M. Nano, M. Degiuli, M. Volante, C. Caccia, V. Leoni, H.R. Griffiths, C.M. Spickett, G. Poli, F. Biasi, Increased production of 27-hydroxycholesterol in human colorectal cancer advanced stage: Possible contribution to cancer cell survival and infiltration, *Free Radical Biology and Medicine* (2019), doi: <https://doi.org/10.1016/j.freeradbiomed.2019.03.020>.

This is a PDF file of an unedited manuscript that has been accepted for publication. As a service to our customers we are providing this early version of the manuscript. The manuscript will undergo copyediting, typesetting, and review of the resulting proof before it is published in its final form. Please note that during the production process errors may be discovered which could affect the content, and all legal disclaimers that apply to the journal pertain.





ACCEPTED

Increased production of 27-hydroxycholesterol in human colorectal cancer advanced stage: possible contribution to cancer cell survival and infiltration.

Rossin D.^a, Dias IHK.^b, Solej M.^c, Milic I.^b, Pitt A.R.^b, Iaia N.^a, Scoppapietra L.^a, Devitt A.^b, Nano M.^a, Degiuli M.^c, Volante M.^c, Caccia C.^d, Leoni V.^e, Griffiths H.R.^f, Spickett C.M.^b, Poli G.^a, Biasi F.^a

Affiliations

^a Dept. of Clinical and Biological Sciences, San Luigi Hospital, Orbassano (Turin), University of Turin, Italy

^b Aston Research Centre for Healthy Ageing, School of Life and Health Sciences, Aston University, Birmingham, UK

^c Dept. of Oncology, San Luigi Hospital, Orbassano (Turin), University of Turin, Italy

^d Genetics of Neurodegenerative and metabolic Diseases, Dept. of Applied Diagnostic, Fondazione IRCCS Istituto Neurologico Carlo Besta, Milan, Italy

^e Department of Laboratory Medicine, University of Milano-Bicocca, School of Medicine, Hospital of Desio, Desio (Milan), Italy

^f Health and Medical Sciences, University of Surrey, Guildford, UK

Authors e-mail addresses: Daniela Rossin, d.rossin@unito.it; IrundikaDias, h.k.i.dias1@aston.ac.uk; Mario Solej, mario.solej@unito.it; Ivana Milic, i.milic@aston.ac.uk; Andrew R. Pitt, a.r.pitt@aston.ac.uk; Noemi Iaia, noemi.iaia@unito.it; Lara Scoppapietra, lara.scoppapietra@edu.unito.it; Andrew Devitt, a.devitt1@aston.ac.uk; Mario Nano, marionano.md@gmail.com; Maurizio Degiuli, maurizio.degiuli@unito.it; Marco Volante, marco.volante@unito.it; Claudio Caccia, claudio.caccia@istituto-besta.it; Valerio Leoni, valerioleoni@hotmail.com; Helen R. Griffiths, h.r.griffiths@surrey.ac.uk; Corinne M. Spickett, c.m.spickett@aston.ac.uk; Giuseppe Poli, giuseppe.poli@unito.it; Fiorella Biasi, fiorella.biasi@unito.it.

Corresponding author:

Fiorella Biasi

Department of Clinical and Biological Sciences, University of Turin at San Luigi Gonzaga Hospital, 10043 Orbassano (Turin), Italy

Phone number: 00390116705420; Fax number: 00390116705424

E-mail: fiorella.biasi@unito.it

Declarations of interest: none

ABSTRACT

So far, the investigation in cancer cell lines of the modulation of cancer growth and progression by oxysterols, in particular 27-hydroxycholesterol (27HC), has yielded controversial results. The primary aim of this study was the quantitative evaluation of possible changes in 27HC levels during the different steps of colorectal cancer (CRC) progression in humans. A consistent increase in this oxysterol in CRC mass compared to the tumor-adjacent tissue was indeed observed, but only in advanced stages of progression (TNM stage III), a phase in which cancer has spread to nearby sites. To investigate possible pro-tumor properties of 27HC, its effects were studied *in vitro* in differentiated CaCo-2 cells. Relatively high concentrations of this oxysterol markedly increased the release of pro-inflammatory interleukins 6 and 8, monocyte chemoattractant protein-1, vascular endothelial growth factor, as well as matrix metalloproteinases 2 and 9. The up-regulation of all these molecules, which are potentially able to favor cancer progression, appeared to be dependent upon a net stimulation of Akt signaling exerted by supra-physiological amounts of 27HC.

Key words: oxysterols, 27-hydroxycholesterol, colorectal cancer, Akt, survival signaling, inflammation, MMP.

Funding: This work was supported by the University of Turin, Italy [grant numbers POLG_RILO_16_01, 2016; BIAF_RILO_17_01], the European Union's Horizon 2020 research and innovation program under the Marie Skłodowska-Curie [grant agreement number 675132], and Biotechnology and Biological Sciences Research Council [grant number BB/M006298/1].

List of abbreviations

24HC, 24-hydroxycholesterol; **25HC**, 25-hydroxycholesterol; **27HC**, 27-hydroxycholesterol; **7 β HC**, 7 β -Hydroxycholesterol; **7K**, 7-ketocholesterol; **AR**, Androgen Receptor; **AT**, adjacent tissue; **Bax**, Bcl-2-associated x; **Bcl**, B-cell lymphoma; **BHT**, butyl hydroxytoluene; **CYP27A1**, 27-hydroxylase; **CRC**, colorectal cancer; **DAPI**, 4',6-diamidino-2-phenylindole; **DMEM**, Dulbecco's modified Eagle's medium; **DPI**, diphenyliodonium; **ECL**, Enhanced chemiluminescence; **ELISA**, Enzyme Linked Immunosorbent Assay; **ER**, Estrogen Receptor; **FBS**, Fetal bovine serum; **FW**, fresh weight; **HPLC/MS**, High Performance Liquid Chromatography/Mass spectrometry; **HRP**, Horseradish peroxidase; **IL**, Interleukin; **LDH**, Lactate dehydrogenase; **MCP**, Monocyte Chemoattractant Protein; **MMP**, Matrix Metalloproteinase; **MTT**, tetrazolium dye 3-(4,5-dimethylthiazol-2-yl)-2,5-diphenyltetrazolium bromide; **NF- κ B**, Nuclear Factor- κ B; **OCT**, Optimum cutting temperature; **Oxy-mix**, Oxysterols mixture; **PBS**, phosphate buffered saline; **PI3K**, phosphatidylinositol-4,5-bisphosphate 3-kinase; **PIP3**, phosphatidylinositol-3,4,5-trisphosphate; **PTEN**,

phosphatase and tensin homolog; **SD**, Standard Deviation; **SDS**, Sodium dodecyl sulphate; **SPE**, Solid phase extraction; **TBS**, tris-buffered saline; **TT**, tumor tissue; **TBST**, TBS-Tween 20; **TEER**, Transepithelial electrical resistance; **VEGF**, vascular endothelial growth factor; **ZO-1**, Zonula occludens-1.

ACCEPTED MANUSCRIPT

1. Introduction

An increasing number of reports are increasingly clarifying the role of oxysterols, a family of cholesterol oxidation products, in human pathophysiology. In particular, side chain oxysterols, which mostly have enzymatic origin, can contribute to a large number of physiological processes [1, 2]. Conversely, it is also widely accepted that a supra-physiological accumulation of oxysterols, of both enzymatic and non-enzymatic generation, may be involved in the pathogenesis of different human degenerative diseases, due to their pro-oxidant and pro-inflammatory properties [3]. The most common oxysterol in human plasma is definitely 27-hydroxycholesterol (27HC), which is ubiquitously produced by mitochondrial cholesterol 27-hydroxylase (CYP27A1); its role in human carcinogenesis is still unclear. 27HC has been suggested to favor the progression of breast and prostate cancers owing to its ability to act as a selective estrogen receptor modulator [4]. Like other endogenous oxysterols identified in human melanoma, lung and kidney cancer cell lines, 27HC was hypothesized to exert a tumor-supporting immunosuppressive action [5]. Moreover, 27HC was reported to facilitate the metastasis in the lung of murine breast cancer [6]. However, such a finding was achieved with daily subcutaneous injection of 27HC at a very high concentration (20 mg/kg) during two weeks in tumor bearing animals. Notably, five days of such a strong treatment were not sufficient to induce lung metastasis in a statistically significant way [6].

How oxysterols - particularly 27HC - could modulate cancer cell proliferation and behavior is far from being clarified. In fact, oxysterol action may depend on different factors such as histological type and stage of cancer, oxysterol concentration, different impact of inflammatory cells, and so on. Indeed, despite reports supporting tumor-promoting effects of specific oxysterols, other studies have outlined potential antitumor action of these compounds. A relatively old but comprehensive review by deWeille et al. discussed the two facets of action of enzymatically-derived oxysterols [7]. More recently, *in vitro* studies have shown the inhibitory action of 27HC on proliferation and migration of human gastric HGC-27 cell line [8].

Bearing these controversial findings in mind, we considered it essential to extend our research from experimental tumor models to human malignant tumors. We focused our study on evaluating 27HC content in the tumor mass of colorectal cancer (CRC) at different stages of malignancy, a condition that had not been previously investigated. Moreover, there is consistent evidence for 27HC being able to trigger and sustain survival signaling in different cell lines [9]. Therefore, the possible mechanisms by which this oxysterol could promote intestinal cancer cell survival and invasiveness were investigated in depth.

2. Materials and Methods

2.1. Chemicals

Unless otherwise specified, reagents and chemicals were obtained from Sigma Aldrich (Milan, Italy). Dulbecco's modified Eagle's medium (DMEM) with high glucose content and GlutaMAX™, fetal bovine serum (FBS), high grade methanol and formic acid for High Performance Liquid Chromatography/Mass spectrometry (HPLC/MS) were from Thermo Fisher Scientific Inc. (Monza, Italy). Six-well plates, 96-well plates and Triton X-100 were from VWR International s.r.l. (Milan, Italy). 24HC, 25HC, 27HC, 7-K and 7βHC and deuterated internal standard 24HC-d7, 25HC-d6, 27HC-d6, 7-K-d7 and 7βHC-d7 were from Avanti Polar Lipids (Alabaster, AL, USA). Oasis® HLB Prime cartridges for solid phase extraction (SPE) were from Waters (Milford, MA, USA). Bio-Rad Protein Assay Dye reagent for protein evaluation and Clarity™ Western ECL Blotting Substrates were from Bio-Rad (Milan, Italy). Nitrocellulose membranes were from GE Healthcare (Milan, Italy).

Human IL-6 ELISA (Enzyme-Linked Immunosorbent Assay) kit was from PeProtech (DBA Italia s.r.l., Milan, Italy). DuoSet ELISA kit for human IL-8 detection was from R&D System, Space Import Export (Milan, Italy). Human monocyte chemoattractant protein-1 (MCP-1) and vascular endothelial growth factor (VEGF)-A ELISA kits were from Ray Biotech Inc. (Prodotti Gianni S.p.A., Milan, Italy). The primary antibodies were rabbit anti-phospho-Ser473 Akt, anti-Akt, and anti-phosphatase and tensin homolog (PTEN) antibodies, the secondary goat anti-rabbit and horse anti-mouse HRP-linked antibodies were from Cell Signaling Technology (Euroclone S.p.A., Milan, Italy). Mouse anti-MMP-9, mouse anti-B-cell lymphoma (Bcl)-XL and anti-Bcl-2-associated x (Bax) antibodies were purchased from Santa Cruz (Tebu-Bio s.r.l., Milan, Italy). The secondary goat anti-mouse antibody and the EnVision System-HRP using diaminobenzidine as the chromogen was from Dako (Glostrup, Denmark).

2.2. Patient recruitment and tissue specimen handling

Tumor and non-tumor tissues were collected from 26 patients affected by CRC at different stages of malignancy. Patients (15 women, 11 men; age range 45 – 80, median age 71) underwent tumor surgical resection at the Surgical Division of San Luigi Gonzaga University Hospital (Orbassano, Turin, Italy) between 2016 and 2017. The tumor specimens were classified following Dukes' modified Astler-Coller and TNM classification. Patients' exclusion criteria: 1) patients aged above 80 or below 40 years old; 2) patients affected by other chronic inflammatory diseases; 3) patients who had undergone previous gut surgical intervention; 4) patients, who had received radiotherapy or chemotherapy before surgery.

Tissues were surgically removed, and specimens were fixed in 4% formaldehyde and then in paraffin for the histopathological analyses. Parts of the specimens were embedded in the optimum cutting temperature (OCT) matrix, frozen and preserved to perform chromatographic analysis on tissue homogenates. In particular, two tissue samples were considered for each patient: 1) Tumor tissue (TT); 2) tumor-surrounding non-tumor tissue (adjacent tissue - AT).

This study was carried out in accordance with The Declaration of Helsinki, approved by the local Ethical Committee (San Luigi Hospital, Orbassano, Italy, MNGP2014) and written informed consent was obtained from each patient enrolled.

2.3. Human cancer cell line culture and treatment

The human colorectal adenocarcinoma CaCo-2 cell line was obtained from Cell Bank Interlab Cell Line Collection (Genoa, Italy). CaCo-2 cells (passages 15-20) were cultured 1×10^6 /ml density in 6-well plates in DMEM GlutaMAX™ supplemented with 10% heat-inactivated FBS, 1% antibiotic/antimycotic solution (100 U/mL penicillin, 0.1 mg/mL streptomycin, 250 ng/mL amphotericin B and 0.04 mg/mL gentamicin) at 37°C and 5% CO₂ in a humidified atmosphere. CaCo-2 cells were cultured for 18 days, and cell medium was replaced three times a week to allow their spontaneous differentiation. Differentiated CaCo-2 cells express morphological and functional characteristics of mature small intestinal enterocytes [10].

After overnight serum starvation, the cell medium was replaced with DMEM containing 5% FBS, and differentiated CaCo-2 cells were treated with different concentrations of 27HC (molecular weight: 402.663 g/mol) at 37°C for different times (3, 6, 12, 24, 48 or 72 hours) for the evaluation of cytotoxicity. The oxysterol concentrations of 1 μM or 5 μM were further chosen to investigate inflammatory and survival signals. In some experiments, cells were pre-treated with different concentrations of PI3K inhibitor LY294002 for 1 hour.

2.4. Quantification of oxysterols by LC-MS/MS

Frozen tissue (100 mg) was ground using a pestle and mortar; powdered samples were collected and re-suspended in 500 μl ice-cold methanol containing 5 mg/ml butyl hydroxytoluene (BHT) (corresponding to 20% tissue homogenate w/v) and incubated for 40 minutes in ice. Samples were then centrifuged (1862 RCF at 4°C for 15 minutes) and the collected supernatants were dried out by using Christ RVC 2-18 vacuum concentrator (Osterode am Herz, Germany). Dried samples were re-suspended with 12.5 % methanol in acidic water with 1% formic acid (v/v). Tissue samples were spiked with deuterated internal standards related different oxysterols. Sterols were extracted by using SPE cartridges and analyzed by liquid chromatography UltiMate 3000 HPLC (Dionex, Thermo Scientific Ltd., Hemel Hempstead, UK) coupled on-line with a ESI-QqLIT-MS/MS mass spectrometer (QTrap 5500, AB Sciex, Warrington, UK) following the protocol used by Dias and colleagues [11]. Multiple reaction monitoring with transitions of 385.4/161 for 27HC and 391.4/135 for the 27-hydroxycholesterol-d6 standard were used. Data files (.wiff format) were examined using Analyst Software 1.7 (AB Sciex, Warrington, UK). Oxysterol tissue content was expressed as ng/g fresh weight (FW) intestinal tissue.

2.5. Evaluation of cell death and proliferation

Cell death was analyzed by extracellular lactate dehydrogenase (LDH) release in cell medium. LDH enzymatic activity was evaluated spectrophotometrically, recorded as Δ Abs/minute at 340 nm wavelength, and reported as a percentage of LDH total release into cell medium when 0.5% Triton X-100 was added to culture flask containing the same cell density as the test sample. A time-course analysis from 3 to 72 h cell treatment with increasing 27HC concentrations was performed.

The tetrazolium dye 3-(4,5-dimethylthiazol-2-yl)-2,5-diphenyltetrazolium bromide (MTT) test was also used for measuring cell proliferation, testing for cytotoxicity related to the number of viable cells upon 27HC treatment [12]. The cells were seeded in 96 well culture plates (1200 cells/well) and incubated with 27HC at different times (3 to 72 hours). After cell treatment with 27HC, 20 μ l MTT from stock solution (5 mg/ml) were added to medium and cells were kept into CO₂ incubator in the dark for 4 h. Formazan crystals were dissolved by replacing medium with 120 μ l DMSO, and the plates incubated for 30 minutes. Purple formazan products was recorded at 550 nm wavelength by using a multiwell plate reader (Model 680 Microplate Reader, Bio-Rad, Milan, Italy), and the absorbance at 655 nm was considered as reference value. Therefore, increased absorbance reflects an increase in the number of viable cells, while its reduction indicates an oxysterol cytotoxic effect in terms of loss of number of cells.

2.6. Immunoblotting

Differentiated CaCo-2 cells were collected in ice-cold lysis buffer (20 mM Tris-HCl, 150 mM NaCl, 1% sodium deoxycholate, 1% Triton X-100, 0.1% SDS, pH 7.4; 0.7 mM AEBSF, 2 mM EDTA, 2 mM EGTA, 50 μ M Leupeptin, 1 μ M Pepstatin, 10 μ M Bestatin, 10 μ M E-64, 1 μ M PMSF and 0.15 unit/ml Aprotinin as protease inhibitors; 5 mM Sodium fluoride, 0.1 mM Sodium orthovanadate, 1 mM Sodium Pyrophosphate and 1 mM β -Glycerophosphate), incubated at 4°C for 20 minutes and centrifuged at 1862 RCF at 4°C for 15 minutes. Total cell lysate protein concentration was evaluated by Bio-Rad protein assay dye reagent [13].

Sample immunoprecipitation (80 μ g protein) was carried out overnight with rabbit anti-Akt monoclonal antibody (4 μ l) only for Akt and pAkt protein level evaluation. Immunoprecipitation was achieved by 2 hours incubation at 4°C with Protein A - Sepharose resin, and pellets were used for immunoblotting analyses.

All samples (immunoprecipitated and not) were boiled at 100°C for 5 minutes in Laemmli buffer [200 mM Tris-HCl, pH 7.4, glycerol 36% (v/v), SDS 7% (w/v), 1M 2-mercaptoethanol, bromophenol blue 0.1% (w/v)] and separated on 10% SDS-polyacrylamide gel electrophoresis (PAGE) (20 μ g/lane), followed by blotting onto Hybond ECL nitrocellulose membranes. The membrane was then blocked in Tris-buffered saline (TBS) with Tween 20 (TBST) [20

mM Tris-HCl (pH 7.6) TBS, 0.1% (v/v) Tween 20] containing 5 % skimmed milk powder (w/v) for 1 hour at room temperature, followed by three 5 minutes washes in TBST.

Blots were then incubated with rabbit anti-Akt (1:1000 dilution), rabbit anti-pAkt Ser473 (1:1000 dilution), rabbit anti-PTEN (1:1000 dilution), mouse anti-Bcl-xL (1:1000 dilution), or mouse anti-Bax (1:1000 dilution) monoclonal antibodies in 5% dry milk – TBST overnight at 4°C on a three-dimensional rocking table.

Blots were washed twice for 10 minutes in TBST and then incubated with goat anti-rabbit/mouse HRP-conjugated secondary antibodies (1:5000 dilutions) for 1 hour in TBST containing 3% skimmed milk powder (w/v). After two further washes with TBST for 10 minutes, blots were exposed to ECL® reagent for 5 minutes following the protocol as described by the manufacturer. Blots were then exposed to Hyperfilm-ECL using a ChemiDoc MP system (Biorad Laboratories, Inc.). Normalization was performed by using β -actin as control reference. Protein bands were quantified through densitometry by using Image J 1.42q software (USA, <http://rsb.info.nih.gov/ij/>). Results were expressed as fold-increase compared to the values obtained in the medium from untreated cells (control).

2.7. Gelatin zymography

Matrix metalloproteinase (MMP)-2 and MMP-9 activation was assessed in the cell incubation medium by gelatin zymography following standard protocols [14]. Cell medium (10 μ g protein) from each sample was diluted in non-reducing Laemmli buffer (8 μ l) and loaded onto 8% SDS polyacrylamide gels containing 0.8 mg/ml gelatin, which acts as substrate for MMP activity. After gel protein separation by electrophoresis, the gels were washed in a renaturing buffer (2.5% Triton X-100 in 50 mM Tris-HCl, pH 7.5, final solution) for 1 hour to allow protein re-fold into native conformation. Gels were then incubated overnight at 37°C in a proteolysis buffer (40 mM Tris-HCl, 200 mM NaCl, 10mM CaCl₂, 0.02% NaN₃, pH 7.5, final solution), then stained for 3 hours in a Coomassie Blue solution (0.05% Coomassie Brilliant Blue R-250, 50% methanol, 10% acetic acid, final solution) and destained with 5% methanol and 7% acetic acid (final solution). The final zymogram showed MMP proteolytic activity as clear bands (cleaved gelatin) on a blue background (uncleaved gelatin). Densitometric analysis was used for the detection of gelatinolytic action of MMP-2 and -9, and performed through Image J Software (USA). Results were expressed as fold increase compared to values obtained in the medium from untreated cells (control).

2.8. Immunohistochemical analysis

Tissue distribution of MMP-9 was tested on 23 stage II and 23 stage III CRC specimens. Paraffin-embedded tissue was deparaffinized and rehydrated through graded alcohols. Heat-induced antigen retrieval was performed by microwave treatment in citrate buffer (pH 6.0) three times for 5 minutes, followed by cooling for 30 minutes at room temperature.

Endogenous peroxidase activity was quenched by a 15 minutes treatment with 3% hydrogen peroxide. Following 15 minutes incubation in bovine serum in TBST, sections were incubated overnight in a humidified chamber at 4°C in the presence of 1 µg/ml mouse anti-MMP-9 polyclonal antibody. After washing with TBS, slides were incubated for 35 minutes with the secondary anti-mouse antibody. The immune reaction was then revealed with EnVision System-HRP using diaminobenzidine as chromogen. Sections were finally counterstained with hematoxylin, dehydrated through graded alcohols, mounted and examined at a Leica microscope (Leica Microsystems Wetzlar GmbH, Wetzlar, Germany). Staining intensity was evaluated random by two independent observers. A semi-quantitative analysis was expressed as the total percentage histological (H)-score, where both intensity (0, 1+, 2+, and 3+) and the percentage of positive cells - ranging from 0 to 300 - were taken into account and combined.

2.9. Protein level evaluation by ELISA

Protein levels of IL-6, IL-8, VEGF and MCP-1 were detected in the cell culture medium by using commercial ELISA kits (see section 2.1. Chemicals) following the manufacturer's instructions. Sample absorbance values were detected using a multiwell plate reader (Model 680 Microplate Reader, Bio-Rad, Milan, Italy) set to a dual-wavelength mode at 450 and 655 nm, where optical density recorded at 655 was considered as the reference. Data were analyzed by using SlideWrite Plus software (Advanced Graphics Software). The analyses of different cytokines were performed in triplicate and expressed as pg/mg of protein.

2.10. Statistical analyses

Statistical differences among different groups were evaluated using Student's t-test and one-way ANOVA test associated with the Bonferroni's multiple comparison post-test. Data were analyzed with GraphPad Prism 6 software (San Diego, CA, USA) and results were expressed as mean ± Standard Deviation (SD).

3. Results

3.1. Marked 27HC increase in human colorectal cancer at advanced stage of progression. Comparison with the corresponding tumor-adjacent tissue.

To provide evidence of the presence of 27HC at CRC tumor site, we performed chromatographic characterization of different oxysterols in sterol extracts from tumor tissues (TT) and adjacent tissue (AT) specimens obtained from 26 CRC patients at different stages of malignancy undergone surgical resections. Table 1 shows patients' details and tumor staging following TNM and Dukes modified Aster-Coller system classification (3 patients were classified as at stage I, 8 as stage II, 12 as stage III, 3 as stage IV).

LC-MS/MS analyses demonstrated that 27HC was the most common side-chain oxysterol in TT as indicated by a representative LC-MS/MS total ion chromatogram (Figure 1A). In particular, Figures 1B and 1C show scatter plots displaying the distribution of 27HC analyzed in TT and non-tumor AT, respectively. No 27HC differences were evident among the four stages in non-tumor AT (Fig. 1B). On the other hand, a strong 27HC increase was evident in tumor tissues at stage III compared to the others (Fig. 1C).

A more detailed analysis of samples from stages II and III, the two groups with the largest number of patients, was carried out. Figure 1D shows that 27HC median content in tumor tissues at stage III malignancy was significantly increased [76.5 ± 17 ng/g FW (Fresh Weight)] compared with tumors at stage II (34.5 ± 11 ng/g FW) and stage III tumor-adjacent tissues (28.5 ± 18 ng/g FW).

3.2. *In vitro* evidence of 27HC pro-inflammatory effect in differentiated CaCo-2 cells

Based on the observed 27HC increase in specimens at stage III CRC tumor malignancy, the possible tumor-promoting role of this oxysterol in favoring the release of inflammatory cytokines involved in tumor growth was studied.

A set of experiments was performed by treating differentiated CaCo-2 cells with increasing concentrations of 27HC in order to evaluate the ability of oxysterol in inducing IL-6 and IL-8 cell release in culture medium. Figure 2 shows cytokine production upon cell treatment with 1 μ M or 5 μ M 27HC for 24 and 48 hours. Only 5 μ M 27HC induced a significant increase in cytokine release in cell culture medium. The increased production of IL-6 was already significant at 24 hours cell incubation (Fig. 2A), while IL-8 production was also significantly increased at 24 hours and reached a higher level and significance after 48 hours cell treatment (Fig. 2B).

Notably these two concentrations did not show any cytotoxic effect in terms of MTT staining and LDH % cell release (Table S1 supplementary material).

3.3. 27HC stimulates intestinal cell release of active MMP-2 and MMP-9

Matrix metalloproteinases have been demonstrated to play a prominent role in cancer cell invasion and dissemination. They are produced and assembled in the cytoplasm, secreted as zymogen pro-MMPs, and extracellularly activated. We recently demonstrated that a mixture of dietary oxysterols was able to activate MMP-2 and MMP-9, as well as increase IL-8 synthesis in differentiated CaCo-2 cells [15]. Therefore, we tested the ability of the endogenous oxysterol 27HC to induce these two MMPs in the same intestinal cell line treated with 1 μ M or 5 μ M 27HC for 24 and 48 hours. As shown by gelatin zymography analyses, both oxysterol concentrations were able to increase MMP activity at the different times considered. MMP-9 appeared to be activated earlier than MMP-2, as it was significantly increased with the lower oxysterol concentration already after 24 h treatment, compared with controls. The highest significant

enzymatic activation of both MMP-2 and MMP-9 was reached after 48 hours of cell treatment with either 1 μ M or 5 μ M 27HC (Fig. 3). Immunohistochemical analysis of MMP-9, gradually increasing toward the tumor invasion front, supports the concept of MMP-9's importance in metastasis (Fig. 4).

3.4. 27HC induces Akt activation in differentiated CaCo-2 cells.

Elevated activity and phosphorylation of serine/threonine kinase Akt are thought to be required for its role in positively regulating cell survival in various types of cancers, included CRC [16]. Activation directly depends on phosphatidylinositol-4,5-bisphosphate 3-kinase (PI3K), and is negatively regulated by the tumor suppressor phosphatase and tensin homolog deleted on chromosome ten (PTEN), Consequently, to investigate the potential ability of 27HC to modulate Akt activation in differentiated CaCo-2 cells, we evaluated phosphorylated Akt (pAkt) by Western Blotting upon cell treatment with 5 μ M 27HC, as this concentration exerted the strongest inflammatory effects. As reported in Figure 5, a marked Akt activation was observed in terms of pAkt/Akt ratio increase in the intestinal cells incubated for 48 hours with the oxysterol (Fig. 5A). Notably, Akt activation was also studied in undifferentiated CaCo-2 tumor cells that showed high pAkt protein levels already at basal conditions without any treatment (Fig. S1). Such substantial pAkt cell content did not allow us to significantly quantify a further possible increase induced by 27HC. Furthermore, at this degree of dedifferentiation, cells had already acquired autonomous survival mechanisms. PTEN catalyzes phosphatidylinositol-3,4,5-trisphosphate (PIP3) dephosphorylation, thus preventing Akt phosphorylation. Therefore, a decreased ratio of PTEN to pAkt proteins can indicate Akt activation. The observed significant reduction of PTEN protein levels after 48 hours of cell incubation with 5 μ M 27HC in terms of decreased PTEN/pAkt protein ratio (Fig. 5B) confirmed the activation of Akt signaling pathway in our experimental model.

3.5. Akt interaction with 27HC-induced inflammation response

To investigate if the observed Akt signaling activation by 27HC could be involved in mediating pro-inflammatory processes induced by this oxysterol, differentiated CaCo-2 cells were pre-treated for 1 hour with 10 μ M LY294002 and then treated with 5 μ M 27HC for 48 hours. LY294002 is a specific inhibitor of PI3K, the enzyme responsible for Akt phosphorylation. The LY294002 concentration used for CaCo-2 pre-treatment was shown to have no cytotoxic effect (Table S2 - Supplementary materials).

LY294002 was able to prevent cell production of specific cytokines involved in tumor development and progression, as well as the activation of MMPs. In addition to the effect exerted by 27HC cell treatment on IL-6 and IL-8 production

(Fig. 6A-B), increased MCP-1 (Fig. 6C) and VEGF (Fig. 6D) levels were also detected in the culture medium after 48h cell treatment with 5 μ M 27HC, but were abrogated by LY294002. Similarly, the observed oxysterol-dependent increased activity of MMP-2 and MMP-9 was prevented by cell pre-treatment with the PI3K inhibitor (Fig. 6E-F), thus supporting a causative association between 27HC-dependent Akt activation and the observed increased production of inflammatory pro-tumor mediators.

3.6. The effect of 27HC-dependent Akt survival signaling on the regulation of apoptosis

PI3K/Akt survival signaling requires concomitant suppression of apoptosis by inhibiting pro-apoptotic Bcl-2 family proteins through their phosphorylation, as well as promoting the expression of anti-apoptotic proteins. Therefore, the ability of 27HC to activate Akt-dependent signaling pathway was investigated by evaluating changes in cell protein levels of pro-apoptotic Bcl-2 associated X (Bax) and anti-apoptotic B-cell lymphoma-extra-large (Bcl-xL) by Western Blotting analyses. The incubation of differentiated CaCo-2 cells with 5 μ M 27HC for 48 hours significantly reduced pro-apoptotic Bax protein levels, while markedly increasing anti-apoptotic Bcl-xL protein levels (Fig.7). On the other hands, these oxysterol-dependent changes were abolished by cell pre-incubation with PI3K inhibitor LY294002 (Fig. 7A-B). Notably, Figure 7C confirmed the ability of LY294002 to inhibit Akt activation. These findings were supported by MTT test results (Table 2). Indeed, the number of viable cells, in terms of percentage of formazan crystals, was increased after 48 hours incubation with 5 μ M 27HC, while in cell samples pre-treated with LY294002 the cell number was comparable to controls. These data provide evidence to support the role of Akt in mediating pro-survival effects of 27HC on intestinal cell line.

4. DISCUSSION

Until now, 27HC has aroused particular interest for its tumor-promoting role in hormone-dependent cancers because of its property to bind estrogen (ER) [17] and androgen (AR) receptors [18]. A quantitative analysis of 27HC carried out on tumor specimens from ER positive breast cancer patients showed a marked increase of this oxysterol in the tumor mass compared with the normal mammary tissue. It reached the low micromolar range in the tumor tissues even if the concentration showed high variability among the different specimens and was not characterized for cancer staging [17]. Guo and colleagues very recently showed by LC-MS an increase in about three times of 27HC in human gastric carcinoma as to the tumor-adjacent normal gastric mucosa, but again no indications of the clinical stage of the nineteen cancers collected was provided [8].

The evidence that 27HC is increased in CRC tissues and that its presence may be functionally related to tumor progression, was previously missing, so the key aim of the present study was to investigate this. The present report

provides a first overall picture of the actual 27HC amount detectable in human CRC along the stages of malignant progression. It is important to outline that, even if this oxysterol appears to accumulate gradually from TNM stage I to TNM stage III, a statistically significant 27HC increase compared to the corresponding tumor-adjacent normal tissue was only detectable in stage III CRC. Notably, LC-MS/MS analysis led to the detection in the CRC mass of relatively low amounts of other oxysterols than 27HC, either of enzymatic origin, i.e. 25HC and 24HC, or non-enzymatic one, i.e. 7K.

The amount of 27HC measured in the other CRC specimens of different stages was within the concentration range observed in the corresponding samples of adjacent normal mucosa. Hence, with regard to human CRC, these findings would clearly indicate that an accumulation of 27HC takes place at a quite advanced stage of cancer progression. The lack of further rise of 27HC detected in the few available specimens of stage IV CRCs is most likely explained by the extreme dedifferentiation displayed by cancer cells at that stage, implying an almost complete loss of intestinal features. Notably, the reported evidence of a supra-physiological accumulation of 27HC in the CRCs of the advanced stage is consistent with the oxysterol metabolizing enzymes' expression profile, which has been recently detected in the tumor microenvironment from a large number of CRC patients [19]. Besides providing conclusive *in vivo* demonstration of the presence or even accumulation of CYP27A1 in colon cancer cells, that study indicated that patients' survival rate was gradually decreasing with the enhancement of CYP27A1 expression [19].

In relation to this, Baek and coworkers showed in an established mouse model of breast cancer that the pro-metastatic effect of a high-cholesterol diet required the presence of CYP27A1 [6].

Evidence for a link between tumors and inflammation has been getting stronger over the years [20, 21]. Stage III malignancy is a crucial step in which cancer has spread to nearby tissues, organs and lymph nodes, and shows a metastatic behavior, even if metastases at distant sites are not yet evident. In this stage different inflammatory molecules may contribute to accelerate cancer progression. The *in vitro* experiments here reported aimed to investigate if a net increase in 27HC as observed in the advanced stage of CRC could give growing neoplasia further pro-inflammatory properties.

Of the various pro-inflammatory cytokines, IL-6 and IL-8 do appear to be associated with malignant progression of colorectal cells. In fact, their serum level was shown to rise in CRC patients in direct proportion to the increase of tumor size and invasiveness [22, 23, 24, 25].

Moreover, IL-8 was found to be constitutively over-expressed in highly aggressive human CRC cells [26]. Our present data indicate a marked enhancement of IL-6 and IL-8 protein release by differentiated CaCo-2 cells when they were challenged for 24 or 48 hours with a relatively high concentration 5 μ M 27HC.

A wide variety of other cytokines has been suggested to have a prognostic value for metastatic CRC patients. Chen and colleagues identified seventeen molecules, including IL-8, MCP-1 and VEGF, which could predict the overall post chemotherapy survival of metastatic patients [27]. A moderate but statistically significant MMP-2 and MMP-9 increased activation was induced by 5 μ M 27HC in differentiated CaCo-2 cells after 48 hours incubation at 37°C. A similar stimulation of MCP-1 and VEGF secretion in the culture medium of CaCo-2 cells challenged for 48 hours with 5 μ M 27HC was found. The histological distribution of MMP-9 observed in stage III CRC, where MMP-9 was gradually increasing from the core of the tumor mass outwards and reaches maximum expression at the growth frontline, is noteworthy.

All these molecules are recognized key players in matrix remodeling, type 2 inflammation and neoangiogenesis, which characterize advanced CRC progression and metastasization [28, 29]. Up-regulation of MMP-9 by 27HC (6 μ M) was already reported in a macrophage cell lineage [30], while a net induction of VEGF cell secretion by 27HC (5 μ M) [31] and MMP-9 increased secretion by 27HC (4 μ M) [32] was observed in breast cancer cell lines.

The interplay among different pro-inflammatory molecules induced by 27HC in micromolar amount might contribute to the survival signaling pathway activation, an important mechanism promoting tumor resistance against apoptosis. Such suppressing apoptotic program occurs by enhancing pro-apoptotic Bcl-xL while decreasing anti-apoptotic Bax cell protein levels. Our reported net activation of PI3K/Akt pathway in differentiated CaCo-2 cells with 5 μ M 27HC well supports such hypothesis. About this, a very recent study claimed apparently opposite data concerning Akt modulation by 27HC in undifferentiated CaCo-2 cells, showing Akt signaling down-regulation exerted by this oxysterol [33]. Those findings were actually obtained by using undifferentiated intestinal cancer cells, thus introducing even higher intercellular variability and higher 27HC concentrations (from 10 μ M upward).

The fact that in the differentiated CaCo-2 model system, the prevention of 27HC-induced enhancement of Akt signaling widely inhibited the oxysterol's pro-inflammatory effect, as well as the anti-apoptotic one further highlights the very likely mechanistic implication of this pleiotropic signaling pathway also in colon cancer progression [for a review see 34].

5. CONCLUSIONS

Despite the few quantitative analyses so far available on oxysterol content - particularly 27HC - in human cancer specimens and not simply human cancer cell lines, there is evidence that an excessive amount of this side chain oxysterol might be present in breast cancer [17] and gastric cancer [8]. Our study now provides the first evidence that this is also true in colorectal cancer.

The here reported LC-MS/MS 27HC evaluation in specimens at different CRC stages clearly indicates that 27HC reaches pathological concentrations only in an advanced stage of tumor progression, at least in humans.

A possible increasing tumoral concentration of this or other oxysterols associated with cancer malignancy, as we found in CRC, would be critical for the progression and invasiveness of different cancer types, and should be more thoroughly investigated.

Once a concentration significantly higher than the physiological one is reached, in this case in the intestine, 27HC definitely appears able to contribute significantly to further cancer progression by triggering and sustaining the hyper-activation of pro-inflammatory cytokines, tissue matrix metalloproteinases, anti-apoptotic factors. Our *in vitro* evidence supports a key role of 27HC-enhanced Akt signaling in triggering the late inflammatory response to CRC growth and invasiveness.

6. REFERENCES

1. B.N. Olsen, P.H. Schlesinger, D.S. Ory, N.A. Baker, Side-chain oxysterols: from cells to membranes to molecules, *Biochim Biophys Acta* 1818 (2012) 330–336. <https://doi.org/10.1016/j.bbamem.2011.06.014>.
2. V.M. Olkkonen, O. Béaslas, E. Nissilä, Oxysterols and their cellular effectors, *Biomolecules* 2 (2012) 76–103. <https://doi.org/10.3390/biom2010076>.
3. G. Poli, F. Biasi, G. Leonarduzzi, Oxysterols in the pathogenesis of major chronic diseases, *Redox Biol.* 1 (2013) 125–130. <https://doi.org/10.1016/j.redox.2012.12.001>.
4. G. Marwarha, S. Raza, K. Hammer, O. Ghribi, 27-hydroxycholesterol: A novel player in molecular carcinogenesis of breast and prostate cancer, *Chem. Phys. Lipids* 207 (2017) 108–126. <https://doi.org/10.1016/j.chemphyslip.2017.05.012>.
5. L. Raccosta, R. Fontana, D. Maggioni, C. Lanterna, E.J. Villablanca, A. Paniccia, A. Musumeci, E. Chiricozzi, M.L. Trincavelli, S. Daniele, C. Martini, J.A. Gustafsson, C. Doglioni, S.G. Feo, A. Leiva, M.G. Ciampa, L. Mauri, C. Sensi, A. Prinetti, I. Eberini, J.R. Mora, C. Bordignon, E.R. Steffensen, S. Sonnino, S. Sozzani, C. Traversari, V. Russo, The oxysterol-CXCR2 axis plays a key role in the recruitment of tumor-promoting, Neutrophils, *J. Exp. Med.* 210 (2013) 1711–1728. <https://doi.org/10.1084/jem.20130440>.
6. A.E. Baek, Y.A. Yu, S. He, S.E. Wardell, C.Y. Chang, S. Kwon, R.V. Pillai, H.B. McDowell, J.W. Thompson, L.G. Dubois, P.M. Sullivan, J.K. Kemper, M.D. Gunn, D.P. McDonnell, E.R. Nelson, The cholesterol metabolite 27 hydroxycholesterol facilitates breast cancer metastasis through its actions on immune cells, *Nat. Commun.* 8 (2017) 864. <https://doi.org/10.1038/s41467-017-00910-z>.

7. J. de Weille, C. Fabre, N. Bakalara, Oxysterols in cancer cell proliferation and death, *Biochem. Pharmacol.* 86 (2013) 154–160. <https://doi.org/10.1016/j.bcp.2013.02.029>.
8. F. Guo, W. Hong, M. Yang, D. Xu, Q. Bai, X. Li, Z. Chen, Upregulation of 24(R/S),25-epoxycholesterol and 27-hydroxycholesterol suppresses the proliferation and migration of gastric cancer cells, *Biochem. Biophys. Res. Commun.* 504 (2013) 892–898. <https://doi.org/10.1016/j.bbrc.2018.09.058>.
9. B. Vurusaner, G. Leonarduzzi, P. Gamba, G. Poli, H. Basaga, Oxysterols and mechanisms of survival signaling, *Mol. Aspects Med.* 49 (2016) 8–22. <https://doi.org/10.1016/j.mam.2016.02.004>.
10. T. Lea, Caco-2 Cell Line, in: K. Verhoeckx, P. Cotter, I. López-Expósito, C. Kleiveland, T. Lea, A. Mackie, T. Requena, D. Swiatecka, H. Wichers (Eds.), *The Impact of Food Bioactives on Health: in vitro and ex vivo models*, Springer, Cham (CH), 2015, pp. 103–111.
11. I.H.K. Dias, I. Milic, G.Y.H. Lip, A. Devitt, M.C. Polidori, H.R. Griffiths, Simvastatin reduces circulating oxysterol levels in men with hypercholesterolaemia, *Redox Biol.* 16 (2018) 139–145. <https://doi.org/10.1016/j.redox.2018.02.014>.
12. T.L. Riss, R.A. Moravec, A.L. Niles, S. Duellman, H.A. Benink, T.J. Worzella, L. Minor, Cell Viability Assays, in: G.S. Sittampalam, N.P. Coussens, K. Brimacombe, A. Grossman, M. Arkin, D. Auld, C. Austin, J. Baell, B. Bejcek, J.M.M. Caaveiro, T.D.Y. Chung, J.L. Dahlin, V. Devanaryan, T.L. Foley, M. Glicksman, M.D. Hall, J.V. Haas, J. Inglese, P.W. Iversen, S.D. Kahl, S.C. Kales, M. Lal-Nag, Z. Li, J. McGee, O. McManus, T. Riss, O.J. Jr. Trask, J.R. Weidner, M.J. Wildey, M. Xia, X. Xu, (Eds.), *Assay Guidance Manual*, E-Publishing Inc., Bethesda (MD), 2004, pp. 357–387.
13. M.M. Bradford, A rapid and sensitive method for the quantitation of microgram quantities of protein utilizing the principle of protein-dye binding, *Anal. Biochem.* 72 (1976) 248–254. [https://doi.org/10.1016/0003-2697\(76\)90527-3](https://doi.org/10.1016/0003-2697(76)90527-3).
14. M. Toth, A. Sohail, R. Fridman, Assessment of gelatinases (MMP-2 and MMP-9) by gelatin zymography, *Methods Mol. Biol.* 878 (2012) 121–135. https://doi.org/10.1007/978-1-61779-854-2_8.
15. M. Deiana, S. Calfapietra, A. Incani, A. Atzeri, D. Rossin, R. Loi, B. Sottero, N. Iaia, G. Poli, F. Biasi, Derangement of intestinal epithelial cell monolayer by dietary cholesterol oxidation products, *Free Radic. Biol. Med.* 113 (2017) 539–550. <https://doi.org/10.1016/j.freeradbiomed.2017.10.390>.
16. S.A. Danielsen, P.W. Eide, A. Nesbakken, T. Guren, E. Leithe, R.A. Lothe, Portrait of the PI3K/AKT pathway in colorectal cancer, *Biochim. Biophys. Acta* 1855(2015) 104–121. <https://doi.org/10.1016/j.bbcan.2014.09.008>.

17. Q. Wu, T. Ishikawa, R. Sirianni, H. Tang, J.G. McDonald, I.S. Yuhanna, B. Thompson, L. Girard, C. Mineo, R.A. Brekken, M. Umetani, D.M. Euhus, Y. Xie, P.W. Shaul, 27-Hydroxycholesterol promotes cell-autonomous, ER-positive breast cancer growth, *Cell Rep.* 5 (2013) 637–645. <https://doi.org/10.1016/j.celrep.2013.10.006>.
18. S. Raza, M. Meyer, C. Goodyear, K.D.P. Hammer, B. Guo, O. Ghribi, The cholesterol metabolite 27-hydroxycholesterol stimulates cell proliferation via ER β in prostate cancer cells, *Cancer Cell Int.* 17 (2017) 52. <https://doi.org/10.1186/s12935-017-0422-x>.
19. R. Swan, A. Alnabulsi, B. Cash, A. Alnabulsi, G.I. Murray, Characterisation of the oxysterol metabolising enzyme pathway in mismatch repair proficient and deficient colorectal cancer, *Oncotarget* 7 (2016) 46509–46527. <https://doi.org/10.18632/oncotarget.10224>.
20. A. Mantovani, P. Allavena, A. Sica, F. Balkwill, Cancer-related inflammation, *Nature* 454 (2008) 436–444. <https://doi.org/10.1038/nature07205>.
21. C. Luo, H. Zhang, The Role of Proinflammatory Pathways in the Pathogenesis of Colitis-Associated Colorectal Cancer, *Mediators Inflamm.* 2017 (2017) 5126048. <https://doi.org/10.1155/2017/5126048>.
22. G. Galizia, M. Orditura, C. Romano, E. Lieto, P. Castellano, L. Pelosio, V. Imperatore, G. Catalano, C. Pignatelli, F. De Vita, Prognostic significance of circulating IL-10 and IL-6 serum levels in colon cancer patients undergoing surgery, *Clin. Immunol.* 102 (2002) 169–178. <https://doi.org/10.1006/clim.2001.5163>.
23. J. Kaminska, M.P. Nowacki, M. Kowalska, A. Rysinska, M. Chwalinski, M. Fuksiewicz, W. Michalski, M. Chechlińska, Clinical significance of serum cytokine measurements in untreated colorectal cancer patients: soluble tumor necrosis factor receptor type I—an independent prognostic factor, *Tumour Biol.* 26 (2005) 186–194. <https://doi.org/10.1159/000086951>.
24. F. Biasi, T. Guina, M. Maina, M. Nano, A. Falcone, E. Aroasio, G.M. Saracco, M. Papotti, G. Leonarduzzi, G. Poli, Progressive increase of matrix metalloproteinase-9 and interleukin-8 serum levels during carcinogenic process in human colorectal tract, *PLoS One.* 7 (2012) e41839. <https://doi.org/10.1371/journal.pone.0041839>.
25. J. Zeng, Z.H. Tang, S. Liu, S.S. Guo, Clinicopathological significance of overexpression of interleukin-6 in colorectal cancer, *World J. Gastroenterol.*, 23 (2017):1780–1786. <https://doi.org/10.3748/wjg.v23.i10.1780>.
26. A. Li, S. Dubey, M.L. Varney, B.J. Dave, R.K. Singh, IL-8 directly enhanced endothelial cell survival, proliferation, and matrix metalloproteinases production and regulated angiogenesis, *J. Immunol.* 170 (2003) 3369–3376. <https://doi.org/10.4049/jimmunol.170.6.3369>.
27. Z.Y. Chen, W.Z. He, L.X. Peng, W.H. Jia, R.P. Guo, L.P. Xia, C.N. Qian, A prognostic classifier consisting of 17 circulating cytokines is a novel predictor of overall survival for metastatic colorectal cancer patients, *Int. J. Cancer* 136 (2015) 584–592. <https://doi.org/10.1002/ijc.29017>.

28. J. Kaur, S.N. Sanyal, Diclofenac, a selective COX-2 inhibitor, inhibits DMH-induced colon tumorigenesis through suppression of MCP-1, MIP-1 α and VEGF, *Mol. Carcinog.* 50 (2011) 707–718. <https://doi.org/10.1002/mc.20736>.
29. A.H. Said, J.P. Raufman, G. Xie, The role of matrix metalloproteinases in colorectal cancer, *Cancers (Basel)* 6 (2014) 366–375. <https://doi.org/10.3390/cancers6010366>.
30. S. Gargiulo, P. Gamba, G. Testa, D. Rossin, F. Biasi, G. Poli, G. Leonarduzzi, Relation between TLR4/NF- κ B signaling pathway activation by 27-hydroxycholesterol and 4-hydroxynonenal, and atherosclerotic plaque instability, *Aging Cell* 14 (2015) 569–581. <https://doi.org/10.1111/ace1.12322>.
31. D. Zhu, Z. Shen, J. Liu, J. Chen, Y. Liu, C. Hu, Z. Li, Y. Li, The ROS-mediated activation of STAT-3/VEGF signaling is involved in the 27-hydroxycholesterol-induced angiogenesis in human breast cancer cells, *Toxicol. Lett.* 264 (2016) 79–86. <https://doi.org/10.1016/j.toxlet.2016.11.006>.
32. Z. Shen, D. Zhu, J. Liu, J. Chen, Y. Liu, C. Hu, Z. Li, Y. Li, 27-Hydroxycholesterol induces invasion and migration of breast cancer cells by increasing MMP9 and generating EMT through activation of STAT-3, *Environ Toxicol Pharmacol.* 51 (2017) 1–8. <https://doi.org/10.1016/j.etap.2017.02.001>.
33. J. Warns, G. Marwarha, N. Freking, O. Ghribi, 27-hydroxycholesterol decreases cell proliferation in colon cancer cell lines, *Biochimie* 153 (2018) 171–180. <https://doi.org/10.1016/j.biochi.2018.07.006>.
34. F. Janku, T.A. Yap, F. Meric-Bernstam, Targeting the PI3K pathway in cancer: are we making headway?, *Nat. Rev. Clin. Oncol.* 15 (2018) 273–291. <https://doi.org/10.1038/nrclinonc.2018.28>.

Figure legends**Figure 1. LC-MS/MS analysis of 27HC content in the surgically resected tumor tissues from CRC patients.**

The 27HC concentration was detected by LC-MS/MS in tumor-surrounding non-tumor tissue (adjacent tissue: AT) and tumor tissue (TT).

Panel A shows a representative LC-MS/MS total ion chromatogram of different oxysterols detected in the tumor tissue of a patient at stage III malignancy, underlying 27HC as the main oxysterol produced at this stage. Oxysterol chromatographic separation was recorded for 48 minutes (min) run time based on the fragmentation ion. The comparison between mass spectra and products' retention times with pure standards was obtained as follows: 24HC (385/161: RT = 14.86 min); 25HC (385/147: RT = 15.30 min); 27HC (385/161: RT = 16.05 min); 7 β HC (385/81: RT = 16.85 min); 7-K (401/196: RT = 17.62 min). Ion intensity values are expressed as counts/second (cps).

Panels B and C show the distribution of 27HC concentration values in AT and TT specimens, respectively, at different CRC stages. The levels of 27HC significant increase in TT stage III compared to stage II malignancy (panel C). The horizontal lines in the panels B and C indicate the median tissue concentration.

Panel D shows histograms of 27HC detected concentrations in the stages II and III and their comparison between AT and the corresponding TT. A significant increase was observed in TT at stage III disease progression compared with the corresponding AT. Values are expressed as ng/g FW intestinal tissue. Significantly different versus Stage III TT: **p <0.01; ***p <0.001; n.s.: not significant.

Figure 2. 27HC induces cell release of pro-inflammatory cytokines IL-6 and IL-8.

IL-6 (panel A) and IL-8 (panel B) were evaluated by ELISA test in the culture medium of differentiated CaCo-2 cells treated with 1 μ M or 5 μ M 27HC for 24 or 48 hours. Maximum increase of both interleukins' cell production was reached after 48-hour cell incubation with 5 μ M 27HC. Values are shown as pg/ml interleukin released by cells in the cell culture medium and are referred to means \pm SD of three independent experiments. Significantly different vs. controls: **p <0.01 and ***p <0.001.

Figure 3. 27HC induces the activation of MMP-2 and MMP-9 in differentiated CaCo-2 cells.

CaCo-2 cells were incubated with 1 μ M or 5 μ M 27HC for 24 or 48 hours; the activation of MMP-2 and MMP-9 was evaluated by gel-zymography and expressed as fold increase than controls (untreated cells). Panels A and B show the activation of MMP-2 and MMP-9, respectively. The gelatinolytic activity of MMP-9 was already increased after 24

hours with the lower concentration of the oxysterol. However, both MMPs reached maximal significance after 48 hour of cell incubation with 5 μ M 27HC.

Data are reported as means \pm SD of three independent experiments. Significantly different vs. controls: ** p <0.01 and *** p <0.001.

Figure 4. A representative immunohistochemical view of MMP-9 tumor tissue distribution.

Left panel - The paraffin embedded CRC tissue section at stage III shows a strongest staining for MMP-9 expression that was localized at the invasive front of the tumor mass (black arrows).

Right panel – Histopathological evidence of MMP-9 immunostaining in different tissues from patients at stages II and III CRC malignancy. Data are referred as percentage of staining reported as total percent H-score. For experimental details see section 2.8 in Materials and Methods. The images were visualized with a 10x/0.22 objective by using Digital Microscope DMD Leica, Leica Microsystems, Milan, Italy. Significantly different versus Stage II: ** p <0.01.

Figure 5. 27HC induces Akt phosphorylation in differentiated CaCo-2 cells.

CaCo-2 cells were incubated with 5 μ M of 27HC and Akt and pAkt protein levels were detected by Western Blotting. The Akt signal activation was evaluated until 72 hours of cell incubation with the oxysterol, and expressed as pAkt/Akt ratio (panel A). Protein levels of PTEN tumor suppressor, the main negative regulator of the PI3K-Akt pathway, were also detected by Western Blotting in differentiated CaCo-2 cells treated with 27HC (5 μ M) for 24 and 48 hours. The observed significant decreased ratio between PTEN and pAkt protein levels after 48 hours of cell incubation with 5 μ M 27HC confirmed the activation of Akt signaling pathway in our experimental model (panel B).

All values are referred to means \pm SD of three independent experiments. Significantly different vs. time zero: # p <0.05, ## p <0.01; significantly different vs. controls: ** p <0.01.

Figure 6. PI3K inhibitor prevents 27HC ability in inducing pro-tumor inflammatory molecules' release in the cell culture medium.

Cells were treated for 48 hours with 27HC (1 μ M or 5 μ M) and pretreated or not with the PI3K inhibitor LY294002 (10 μ M). The IL-6, IL-8, MCP-1 and VEGF protein levels were assessed by ELISA in the cell medium, and expressed as pg/ml (panels A, B, C and D, respectively). The activation of MMP-2 and MMP-9 was analyzed through gel-zymography and expressed as fold increase than control (panels E and F, respectively). All values are referred to means \pm SD of three independent experiments. Significantly different vs. controls: * p <0.05, ** p <0.01 and *** p <0.001; significantly different vs. 5 μ M 27HC: # p <0.05 and ### p <0.001.

Figure 7. 27HC impairs pro-apoptotic protein levels through Akt activation.

The oxysterol 27HC reduced pro-apoptotic Bax, while markedly increased anti-apoptotic Bcl-xL. Cell pre-treatment with the PI3K inhibitor LY294002 prevented 27HC-dependent changes of the two above-mentioned proteins involved in the apoptosis modulation. Cell protein levels of Bax (panel A) and Bcl-xL (panel B) were determined by Western Blotting in differentiated CaCo-2 cells treated with 5 μ M 27HC for 48 hours, pre-treated or not with 10 μ M PI3K inhibitor LY294002 for 1 hour. Panel C shows the successful inhibition of Akt signal by LY294002. Representative immunoblots of Bax, Bcl-xL, pAkt, Akt (and Actin as reference protein) are shown in panel D. All values represent means \pm SD of three independent experiments. Significantly different vs. controls: *p <0.05 and **p <0.01; significantly different vs. 5 μ M 27HC: #p <0.05 and ##p <0.01.

Table 1. Clinical characteristics of CRC patients

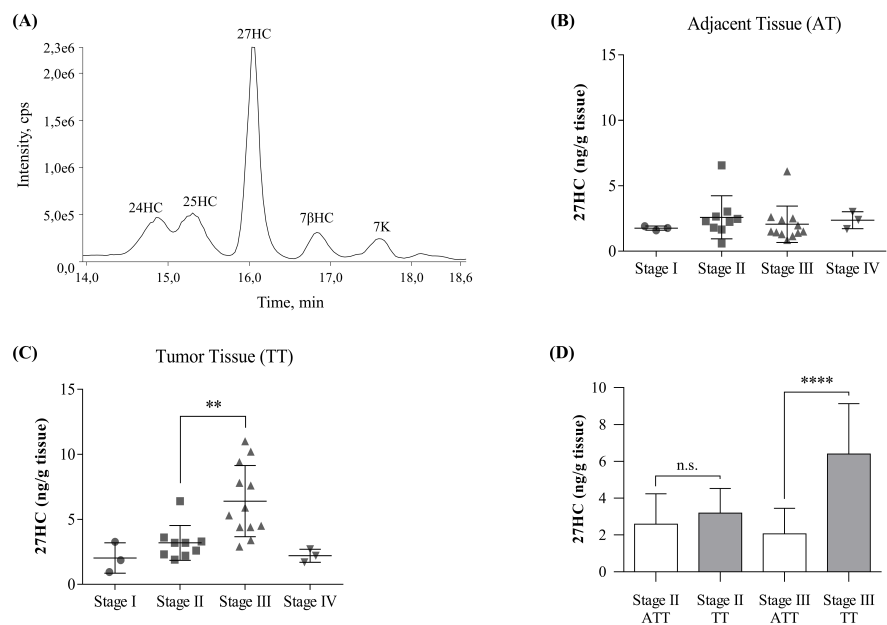
<u>CRC Stages</u>	Number of Patients			
	I	IIA	III (B/C)	IV
	3	8	12 (7/5)	3
<u>Grading</u>				
Low	2	4	4/2	-
Intermediate	1	1	1/-	1
High	-	3	2/3	2
<u>Gender</u>				
Female	1	7	6	1
Male	2	1	6	2
<u>Age (median)</u>				
	76	71.5	78	68
<u>Tumor location</u>				
Right/transverse colon	-	3	7	-
Left colon	3	5	5	3
Rectum	-	1	-	-

Table 2. Analysis of cell viability by MTT test in differentiated CaCo-2 cells pre-treated with LY294002 and treated with 27-hydroxycholesterol.

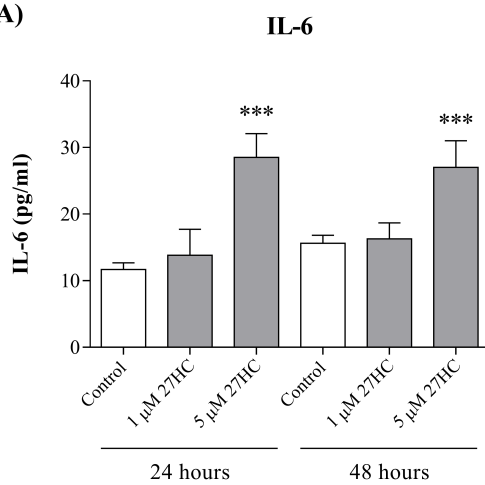
	MTT (% control)
10 μ M LY294002	95 \pm 11
5 μ M 27HC	150 \pm 23*
5 μ M 27HC +10 μ M LY294002	92 \pm 10 [#]

Differentiated CaCo-2 cells were pre-treated with 10 μ M LY294002 for 1 hour, then incubated or not with 5 μ M 27HC for 48 hours. Cell viability was evaluated tetrazolium dye MTT crystals' formation recorded at 550 nm wavelength and was expressed as percentage of control (taken as 100%).

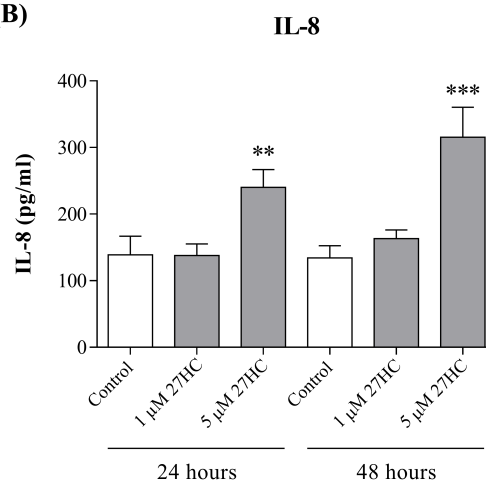
* Significantly different vs. control (untreated cells): $p < 0.05$; # significantly different vs. 5 μ M 27HC treated cells: $p < 0.05$.

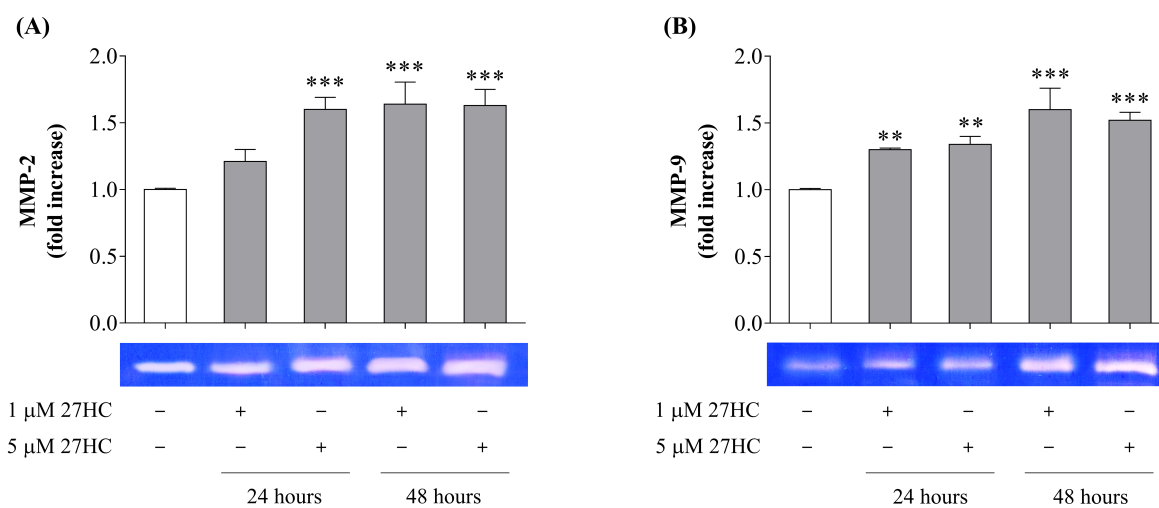


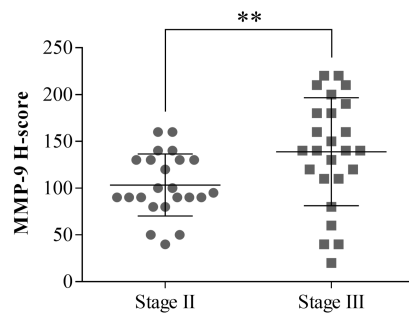
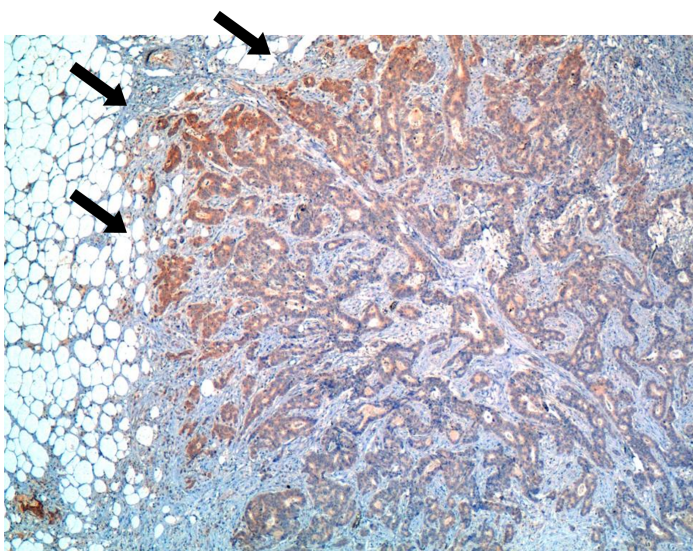
(A)



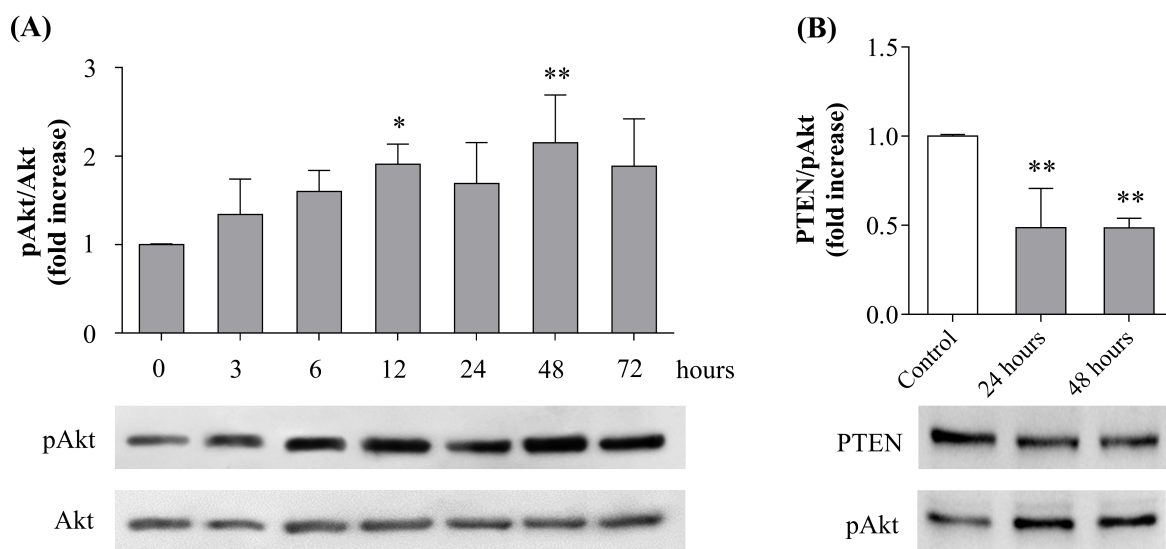
(B)

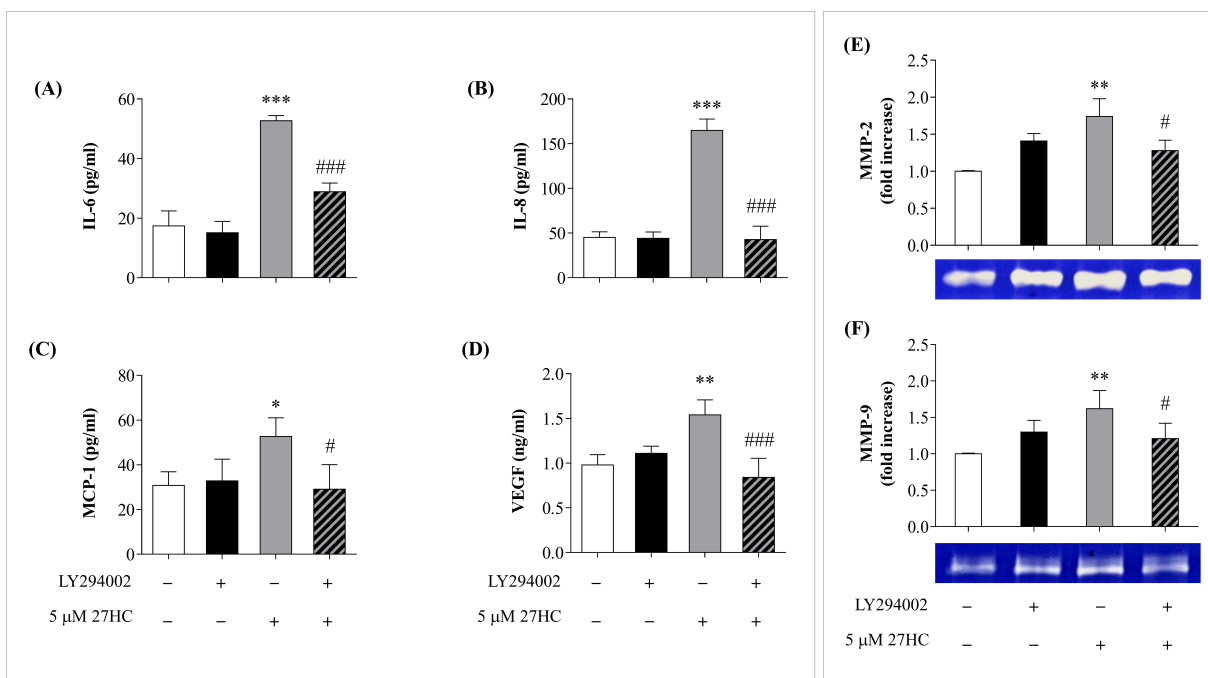




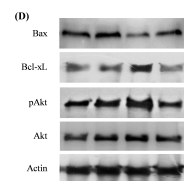
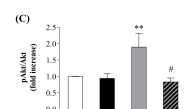
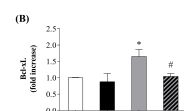
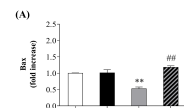


ACCEPTED MANUSCRIPT





ACCEPTED MANUSCRIPT



LY294002	-	+	-	+
5 μM 27HC	-	-	+	+

ACCEPTED MANUSCRIPT

Highlights

- 27-hydroxycholesterol (27HC) is involved in colorectal cancer (CRC) progression
- 27HC reaches high pathological concentrations in CRC advanced stage in humans
- 27HC *in vitro* increases cell release of pro-tumor inflammatory mediators
- 27HC favors survival and invasiveness-related cell signals in intestinal cells